

# Characterization for strontium titanate/Fe<sub>3</sub>O<sub>4</sub> and TiN/Fe<sub>3</sub>O<sub>4</sub> interfaces

A. Lussier<sup>a)</sup> and Y. U. Idzerda

*Department of Physics, 264 EPS Building, Montana State University-Bozeman, Bozeman, Montana 59717*

S. Stadler

*Department of Physics, Southern Illinois University, Carbondale, Illinois 62901*

S. B. Ogale, S. R. Shinde, and V. Venkatesan

*Center for Superconductivity Research, 2117 Physics Building, University of Maryland, College Park, Maryland 20742*

(Received 7 January 2002; accepted 13 April 2002)

The interface formation between different thicknesses of strontium titanate (SrTiO<sub>3</sub>) or titanium nitride (TiN) with a 2000 Å Fe<sub>3</sub>O<sub>4</sub> film is studied using x-ray absorption spectroscopy (XAS) and x-ray magnetic circular dichroism (XMCD). Our results show that the deposition of 10–50 Å of TiN results in an immediate and substantial removal of oxygen from the near interface region, resulting in the formation of spin-randomizing FeO interlayers. For the deposition of SrTiO<sub>3</sub> on Fe<sub>3</sub>O<sub>4</sub>, our measurements show only a small deviation from the Fe<sub>3</sub>O<sub>4</sub> characteristic XAS signature, suggesting the limited formation of perhaps only one monolayer of another Fe oxide at the interface. The persistent XMCD signal, however, confirms the preservation of Fe<sub>3</sub>O<sub>4</sub> in its ferromagnetic state.

© 2002 American Vacuum Society. [DOI: 10.1116/1.1491538]

## I. INTRODUCTION

Half-metallic ferromagnets (HMF) are metals for which the Fermi level falls within one of the spin band gaps.<sup>1</sup> Because the electrons that participate in the conductivity must lie within a few kT of the Fermi level, these materials are recognized as ideal for application in spin conductance device structures.<sup>2,3</sup> Even if HMFs were routinely manufacturable, for use as spin conductance devices, they must be employed as one layer of a multilayered structure.<sup>4,5</sup> For technologically relevant applications, it is essential that the high spin polarization observed in the bulk of a single HMF layer persists throughout the entire multilayer structure and that the interfacial regions do not degrade the electron spin character.

Maintaining the spin character of the electron relies on the magnetic, chemical, and structural characteristics of buried (under a nonmagnetic layer) and hidden (under another magnetic layer) interfaces between the constituent materials. Although the structural and chemical qualities of the interface play an important role in electron transport across the interface, the magnetic properties of the interface determine the electron spin transport properties of the structure and, therefore, the magnetoconductance.<sup>6</sup> A poor quality magnetic interface may degrade the spin transport performance (e.g., it may reduce the electron spin polarization or limit the spin coherence). Furthermore, the magnetic properties of the interface may be very different from those of the bulk due to reduced magnetic coordination, roughness, or interdiffusion, creating magnetic moments that are noncollinear with the bulk and interfering with the transmission of polarized electrons across the interface.

The successful realization of proposed magnetic/semiconductor, magnetic/insulator, and magnetic/metal

structures relies on maintaining the electron spin characteristics as they traverse, or are reflected at interfaces associated with overlayers and/or multilayers. Although Fe<sub>3</sub>O<sub>4</sub> is the prototypical HMF, experimental demonstrations of its half metallicity have not been accomplished due, in part, to the failure to generate a good interface for transport measurements. For these magnetic structures, the overall electron spin transport behavior and device performance depend both on superior materials and controlled magnetic interfaces.

## II. TECHNIQUE

To fully characterize both the quality of the material and the interfaces, we have used x-ray absorption spectroscopy (XAS) and x-ray magnetic circular dichroism (XMCD) on *ex situ* grown Fe<sub>3</sub>O<sub>4</sub> films interfaced to various overlayers that may serve as appropriate interlayer materials. XMCD is a synchrotron based element specific, magnetic spectroscopic tool where absorption spectra for left- and right-hand side circular polarized photons are measured at the absorption edges of the relevant element, and then subtracted from each other.<sup>7,8</sup> Standard XAS is obtained by adding these two polarization dependent spectra. It gives information concerning the chemical state of the element. XMCD gives information concerning the magnetic state of the element.<sup>9</sup>

Figure 1 shows how the x-ray absorption selection rules associated with the XMCD process act on the unique band structure of a HMF. In addition to the helicity-independent dipole selection rule that the angular momentum of the electron must change by  $\pm 1$ , there are selection rules for the magnetic quantum number. For a circular polarization selected so that the photon spin is anti-aligned with the majority spin of the electron (left-hand side of Fig. 1), the appropriate x-ray absorption selection rule is that the magnetic quantum number must change by  $-1$ . For the opposite circular polarization, where the photon spin is aligned with the

<sup>a)</sup>Electronic mail: lussier@physics.montana.edu

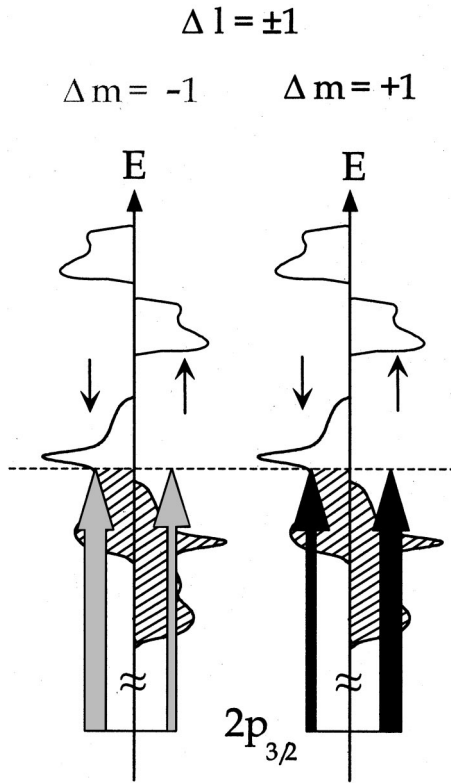


FIG. 1. Effect of the absorption selection rules for circularly polarized x rays aligned (right-hand side) and anti-aligned (left-hand side) to the majority electron spin direction on the HMF band structure.

majority spin of the electrons (right-hand side of Fig. 1), the magnetic quantum number must change by +1. Note that electron transitions occur for both spin subbands (with different probabilities), but due to the absence of one spin state at the Fermi level, the absorption process is spin selective when the photon energy matches an  $L$ -edge binding energy and is mixed at slightly higher or lower photon energies. This has the net effect that, for the transition metal  $L$  edges, the  $L_3$  ( $L_2$ ) edge is increased (decreased) for the anti-aligned case and decreased (increased) for the aligned case. If the two helicity-dependent spectra are summed, the resulting XAS is independent of the electron spin direction, and therefore of the film magnetization also. The XAS spectrum therefore represents the spectrum for *all Fe atoms*. On the other hand, the difference of the two helicity-dependent spectra, the XMCD spectrum, represents the spectrum for *only the ferromagnetic Fe atoms*. In this way, we can separate the contributions of the Fe atoms in ferromagnetic and nonferromagnetic environments to the overall Fe absorption spectra.

### III. EXPERIMENT

To determine the effect of the deposition of an overlayer on a prototypical HMF, we have performed XMCD and XAS experiments at the  $L$  edges of iron in Fe<sub>3</sub>O<sub>4</sub> films with a single TiN or SrTiO<sub>3</sub> (STO) overlayer. Multiple samples with different overlayer thicknesses were grown by pulsed laser deposition at the University of Maryland on MgAl<sub>2</sub>O<sub>4</sub> sub-

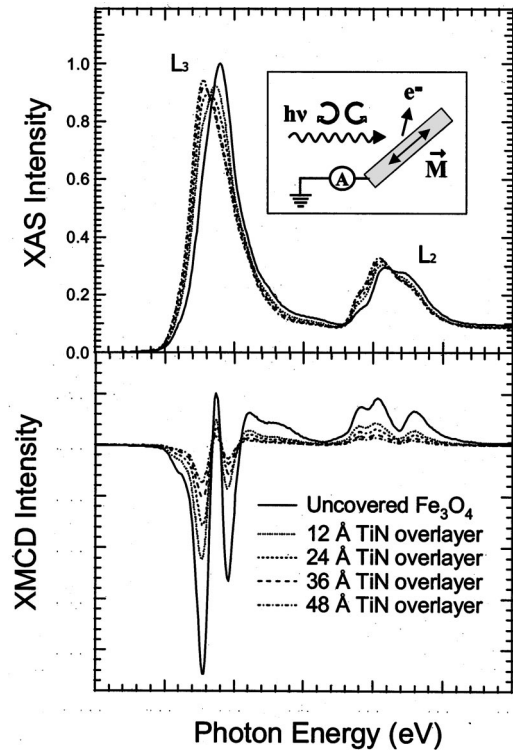


FIG. 2. Peak area normalized Fe  $L_{2,3}$  XAS (top) and XMCD (bottom) spectra as a function of TiN overlayer thickness. The upper inset is the experimental geometry. The XMCD intensity is corrected for incidence angle and incomplete degree of circular polarization of the beam.

strates. Substrate temperatures were 150 °C for the Fe<sub>3</sub>O<sub>4</sub> growth, and 200 °C for the overlayer film growth. The Fe<sub>3</sub>O<sub>4</sub> thickness was 2000 Å for all samples and the overlayer thickness varied from 0 to 48 Å.

The XAS and XMCD spectra were measured at the Montana State University/National Research Laboratory (MSU/NRL) Magnetic Materials X-ray Characterization Facility located at beamline U4B of the National Synchrotron Light Source (NSLS) at Brookhaven National Laboratory. The beamline supplies monochromatic, circularly polarized x rays (in this case, a polarization of 70% was used) in the energy range 20–1350 eV. The monochromator was set at a resolution of 0.25 eV at the Fe  $L_{2,3}$  edges. The details of the U4B beamline have been published elsewhere.<sup>10,11</sup>

We record two total electron yield spectra, one with the incident light helicity (circular polarization) oriented parallel to the remnant magnetization of the sample and one antiparallel, as shown in the inset of Fig. 2. The XAS is the average of these two spectra, while the XMCD is the difference between the two. Here, the light helicity was kept constant while the sample remnant magnetization was reversed at each photon energy by reversing a magnetic field applied in plane with the sample. All XMCD spectra have been corrected for incomplete photon polarization and the 45° sample orientation with respect to the incoming beam.<sup>12</sup> With this experimental configuration, our measurements are sensitive to the top 50–100 Å of the Fe<sub>3</sub>O<sub>4</sub> film. To first order, the presence of the TiN or STO overlayer does not change our

probing depth, but does decrease the signal intensity. The results reported here are therefore not due to any variation of the probed interfacial volume. The spectra were collected at room temperature and at pressures less than  $5 \times 10^{-10}$  Torr. They were normalized to the incident flux via the current measured through a gold mesh placed in the beam prior to the sample.

### A. Overlayer effects on Fe<sub>3</sub>O<sub>4</sub>:TiN

Figure 2 shows the effect of various thickness of TiN overlayer deposition on the peak area normalized Fe  $L_{2,3}$  XAS and XMCD spectra. As the TiN overlayer thickness changes, there is a marked change in the XAS spectra. First, a shoulder appears at lower binding energy (at approximately 707.7 eV if we focus on the  $L_3$  edge), then the spectral weight shifts from the peak toward that shoulder. Simultaneously, the XMCD spectra are observed to decrease in intensity, but remain essentially unchanged in shape. This can only occur if the Fe environment is changing from a ferromagnetic Fe<sub>3</sub>O<sub>4</sub> environment to a nonmagnetic environment with TiN overlayer deposition.

The different binding energies for Fe in different valence states yield a method to differentiate the chemical state of the Fe. Iron in FeO is Fe<sup>2+</sup>, iron in Fe<sub>2</sub>O<sub>3</sub> is Fe<sup>3+</sup>, and iron in Fe<sub>3</sub>O<sub>4</sub> has a mixed valence. We can therefore tell which state of oxidation the iron is in from the position of the Fe XAS  $L$  edge (lower binding energy for Fe<sup>2+</sup>). Figure 2 shows the spectral weight of the  $L_3$  edge shifting from the Fe<sub>3</sub>O<sub>4</sub> position to the FeO position as the thickness of the TiN overlayer is increased from 0 to 48 Å. We conclude that there is a continuous decrease of Fe<sub>3</sub>O<sub>4</sub> in the interfacial region via the formation of FeO. The FeO is the byproduct of oxygen out-diffusion from the Fe<sub>3</sub>O<sub>4</sub> into the TiN (probably forming TiO<sub>2</sub>). Although we were unable to directly monitor the formation of TiO<sub>2</sub> from oxygen absorption at the TiN interface, the relative formation energies for various compounds strongly suggest TiO<sub>2</sub> formation as the most likely occurrence.

### B. Overlayer effects on Fe<sub>3</sub>O<sub>4</sub>:SrTiO<sub>3</sub>

STO has already demonstrated itself to be a high performance interlayer material for oxide bearing ferromagnets and was therefore considered as a candidate material.<sup>9,13</sup> Figure 3 shows the peak area normalized Fe  $L_{2,3}$  XAS and XMCD spectra as a function of STO coverage. Unlike the behavior from TiN overlayers, STO overlayers generate only minor changes in the XAS spectra, and no change in the XMCD spectra (with two notable exceptions). For these two exceptions (the 22 Å and 24 Å STO overlayer thicknesses), we observe a substantially reduced XMCD intensity. The corresponding XAS spectra also exhibit a peculiar trend. Again, for these thicknesses, the observed  $L_3$  edge shift with increasing STO thickness is not a simple shift toward the FeO peak but rather a change in shape. The peak height at the initial position is in fact slightly increased and a clear shoulder appears on the left-hand side of the  $L_3$  edge. This can be easily observed in the enlarged inset to Fig. 3. The reason for

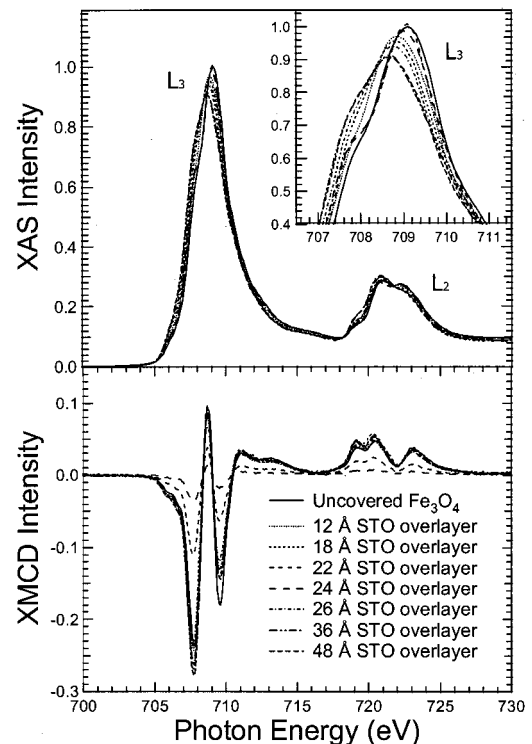


FIG. 3. Peak area normalized Fe  $L_{2,3}$  XAS (top) and XMCD (bottom) spectra as a function of STO overlayer thickness. The upper inset is an enlargement of the  $L_3$  peak for detail. The XMCD intensity is corrected for incidence angle and incomplete degree of circular polarization of the beam.

this XAS and XMCD behavior may be due to a magnetic reorientation, perhaps from a structural transition as the film thickness reaches approximately 22 Å. Additional work should be done to complement our preliminary results in this thickness range.

Additional insight into the overlayer effect on the Fe<sub>3</sub>O<sub>4</sub> can be determined from the overlayer thickness dependence of the XMCD peak intensity, as displayed in Fig. 4. For the TiN data, we see an exponential decrease of the Fe<sub>3</sub>O<sub>4</sub> component with increased overlayer thickness. This type of decay is suggestive of a single dominant barrier to FeO forma-

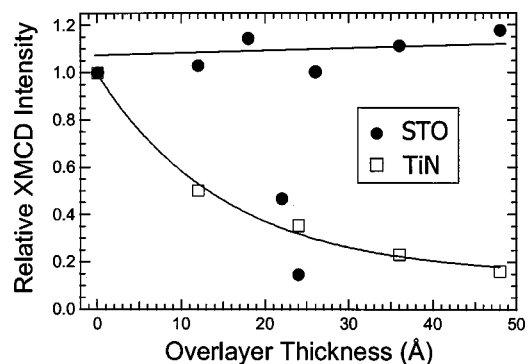


FIG. 4. Fe  $L_3$  peak XMCD intensity for TiN (open squares) and STO (filled circles) as a function of overlayer thickness. The line represents a least-squares fit through the data points for an exponential (TiN) and linear (STO) fit.

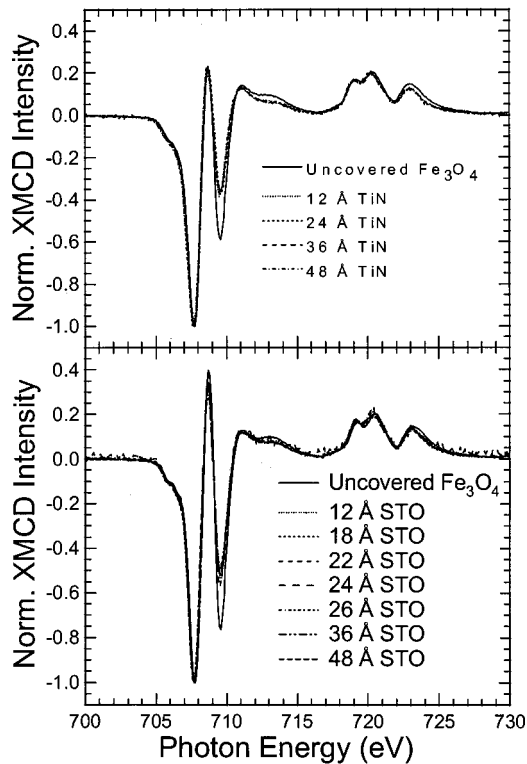


FIG. 5. Fe  $L_{2,3}$  XMCD spectra all separately normalized to the first peak intensity for TiN (top panel) and SrTiO<sub>3</sub> (bottom panel) for all overlayer thicknesses.

tion. Furthermore, the XMCD intensity is only sensitive to the ferromagnetic iron and is therefore a direct measure of it. The STO data shows a constant XMCD intensity (except for the two thicknesses previously discussed).

To confirm that the XMCD spectra are direct indicators of the percentage of Fe<sub>3</sub>O<sub>4</sub> in the interfacial region, in Fig. 5, we show all XMCD spectra after normalization to the peak-to-peak intensity. In each case, all STO and TiN samples have exactly the same shape. There is a slight deviation when compared to the uncovered Fe<sub>3</sub>O<sub>4</sub> films, but this may be due to a degradation of the uncapped films upon transport from the growth chambers, through extended periods of time in air, to the XMCD characterization chamber. It should be noted that the uncovered films used for comparison in the TiN and STO studies have slightly different XMCD spectra. This may represent growth variations from sample to sample, or these two uncovered samples may have experienced varying levels of exposure to air between growth and characterization, leading to slightly varying spectra.<sup>14</sup>

Still, we are confident that the Fe XMCD relative intensity is a direct measure of the percentage of Fe<sub>3</sub>O<sub>4</sub> in the interfacial region. A further check of this conclusion can be made. By taking this percentage decrease in the XMCD intensity (relative to the uncovered Fe<sub>3</sub>O<sub>4</sub> XMCD intensity), we can determine the fraction of Fe<sub>3</sub>O<sub>4</sub> lost due to oxygen outdiffusion attributed to the addition of the overlayer. Knowing this, we can scale the uncovered Fe<sub>3</sub>O<sub>4</sub> XAS spectra by this determined percentage and subtract this reduced

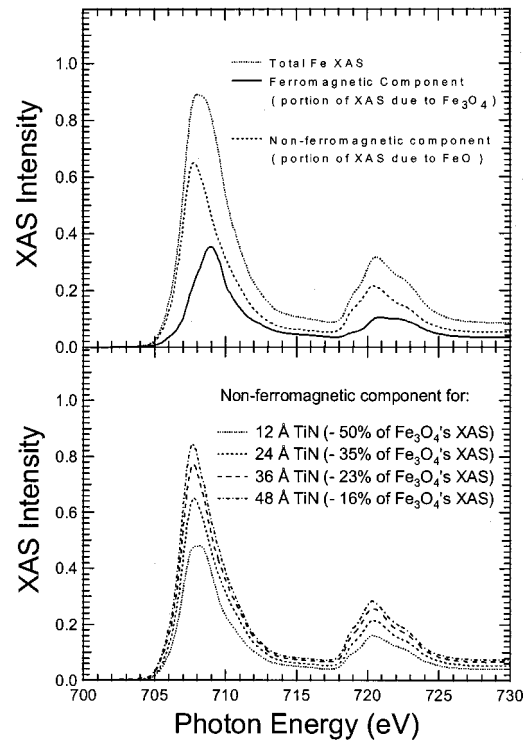


FIG. 6. Top panel: The Fe  $L_{2,3}$  XAS for the 12 Å TiN overlayer sample (dotted line), the scaled Fe  $L_{2,3}$  XAS for the uncapped Fe<sub>3</sub>O<sub>4</sub> (solid line), and the resulting spectra from the subtraction process (dashed line). Bottom panel: Remaining component of the Fe  $L_{2,3}$  XAS spectra for all TiN overlayer thicknesses after subtraction.

Fe<sub>3</sub>O<sub>4</sub> contribution from the total measured XAS spectrum to obtain the residual spectrum representative of the nonmagnetic Fe component for identification purposes. Following this procedure for all TiN overlayer thicknesses consistently yields the same spectrum, corresponding to the XAS spectrum for Fe in FeO. The procedure and results are portrayed in Fig. 6.

Finally, as a check, this same subtraction procedure can be applied to the two STO thicknesses that resulted in the greatly reduced Fe XMCD intensities (22 Å and 24 Å). This procedure, shown in Fig. 7, results in two spectra which are very different from the FeO spectra of Fig. 6, but similar to

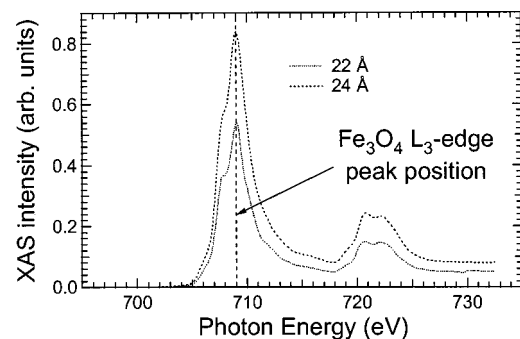


FIG. 7. Remaining Fe  $L_{2,3}$  XAS spectra for two STO overlayer thicknesses after subtraction process. The major peak is still aligned to the Fe<sub>3</sub>O<sub>4</sub> peak position (dashed line).

the Fe<sub>3</sub>O<sub>4</sub> spectra. This is good evidence that in this case, the reduction in XMCD intensity is not the result of Fe<sub>3</sub>O<sub>4</sub> converting to FeO, but a change in the remnant magnetic state of the Fe. The chemical state of the Fe is not altered by the STO overlayer, but a change in the magnetic state of the Fe may occur at a critical thickness of  $\sim 25$  Å.

#### IV. CONCLUSIONS

We conclude that the deposition of titanium nitride on Fe<sub>3</sub>O<sub>4</sub> disrupts the interface via the formation of FeO, and the concurrent loss of magnetization, rendering it an unsuitable interlayer material for Fe<sub>3</sub>O<sub>4</sub> based multilayer magnetoconductive devices. Our preliminary results on STO support the idea that it preserves the Fe<sub>3</sub>O<sub>4</sub> film intact, thus proving to be a promising alternative for interlayer materials.

#### ACKNOWLEDGMENTS

Experiments were conducted at the MSU/NRL Magnetic Materials X-ray Characterization Facility located at the U4B beamline of the NSLS. Joe Dvorak assisted in some of the x-ray measurements. This work was supported by ONR (A. Lussier, Y. Idzerda, and S. Stadler) and NSF-MRSEC DMR 00-80008 (S. Ogale, S. Shinde, and V. Venkatesan). NSLS is supported by DOE.

- <sup>1</sup>R. A. de Groot, F. M. Mueller, P. G. van Engen, and K. H. J. Buschow, *Phys. Rev. Lett.* **50**, 2024 (1983).
- <sup>2</sup>G. A. Prinz, *Phys. Today* **48**, 58 (1995).
- <sup>3</sup>G. A. Prinz, *Science* **282**, 1660 (1998).
- <sup>4</sup>B. Dieny, V. S. Speriosu, S. S. Parkin, D. R. Wilhoit, K. P. Roche, S. Metin, D. T. Peterson, and S. Nadimi, *Phys. Rev. B* **43**, 1297 (1991).
- <sup>5</sup>J. Z. Sun, W. J. Gallagher, P. R. Duncombe, L. Krusin-Elbaum, R. A. Altman, A. Gupta, Y. Lu, G. Q. Gong, and G. Xiao, *Appl. Phys. Lett.* **69**, 3266 (1996).
- <sup>6</sup>M. Sharma, S. X. Wang, and J. H. Nickel, *Phys. Rev. Lett.* **82**, 616 (1999).
- <sup>7</sup>C. T. Chen, F. Sette, Y. Ma, and S. Modesti, *Phys. Rev. B* **42**, 7262 (1990).
- <sup>8</sup>Y. U. Idzerda, C.-T. Chen, H.-J. Lin, G. Meigs, G. H. Ho, and C.-C. Kao, *Nucl. Instrum. Methods Phys. Res. A* **347**, 134 (1994).
- <sup>9</sup>S. Stadler, Y. U. Idzerda, Z. Chen, S. B. Ogale, and T. Venkatesan, *Appl. Phys. Lett.* **75**, 3384 (1999).
- <sup>10</sup>S. Hulbert, D. J. Holly, F. H. Middleton, and D. J. Wallace, *Nucl. Instrum. Methods Phys. Res. A* **291**, 343 (1990).
- <sup>11</sup>Y. U. Idzerda, V. Chakarian, and J. W. Freeland, *Synchrotron Radiat. News* **10**, 6 (1997).
- <sup>12</sup>V. Chakarian, Y. U. Idzerda, and C. T. Chen, *Phys. Rev. B* **57**, 5312 (1998).
- <sup>13</sup>J. M. DeTeresa, A. Barthelemy, A. Fert, J. P. Contour, F. Montaigne, and P. Seneor, *Science* **286**, 507 (1999).
- <sup>14</sup>For consistency, all samples in the two groupings (STO capping and TiN capping) were made together, but the two groups of samples were made months apart.